Int J Clin Exp Pathol 2015;8(10):12014-12027
www.ijcep.com /ISSN:1936-2625/IJCEP0014793

Original Article

Angiogenesis dependent characteristics of tumor observed on rabbit VX_2 hepatic carcinoma

Liming Guan

Department of Obstetrics and Gynaecology, Zhabei District Central Hospital, No. 619, Zhonghuaxin Road, Zhabei District, Shanghai 200000, China

Received August 20, 2015; Accepted September 24, 2015; Epub October 1, 2015; Published October 15, 2015

Abstract: Objective: To evaluate angiogenesis dependent characteristics of carcinoma proliferation, metastasis and to found if there is tumor vascularity architecture defect. Methods: 36 rabbits were random divided into 2 groups: Experimental group: 18 rabbits liver were implanted with VX_2 tumor by surgery operation; Control group: 18 experimental rabbits performed the same surgery operation without tumor implantation, the course of tumor growth and blood vessel invasion was observed by autopsy. One slide was used for hematoxylin-eosin (HE) staining, one slide was used for elastic fiber staining by Victoria blue and Ponceau's histochemical staining, and one slide was used for vascular endothelial cell immunohistochemical staining with biotinylated-ulex europaeus agglutinin I (UEA I); all three slides were observed under an optical microscopic. One additional slide was systematically observed by electron microscopy. SPSS 19.0 software was used for the statistical analyses of the data. Results: The tumor grew acceleration after tumor angiogenesis, volume of original tumors was correlated with vascular caliber. The central tumor found necrosis without enough blood supply while tumor grew rapidly after tumor angiogenesis. The tumor infiltrated into liver blood sinus, blood vessels in hepatic interstitial tissue, the liver capsular vein and important organs metastasis such as lungs, kidneys, abdominal cavity caused rabbits died. The average vascular density count of 18 experimental rabbits under 400 times light microscope were 43.17 ± 8.68/vessels/High Power Field; Tumor vascular diameter all within 200 μm. Vascular elastic fiber staining presented tumor blood vessels internal, external elastic plate intact, vascular endothelial cells organelles of tumor were integrity without endothelial cells architecture defect found by pathologic observation. Conclusion: Proliferation and metastasis of rabbit VX_2 hepatic carcinoma was correlated with tumor angiogenesis and no tumor vascular architecture defect was found by pathologic observation, it need further exploration by other methods.

Keywords: Carcinoma proliferation, metastasis, carcinoma vascularities, vascular density count, tumor angiogenesis

Introduction

Angiogenesis is a complex biological phenomenon that forms new blood vessels from the pre-existing vasculature. Aberrant angiogenesis has been implicated in a variety of diseases such as cancer, atherosclerosis, arthritis, obesity, pulmonary hypertension, diabetic retinopathy, and age-related macular degeneration. These conditions collectively affect nearly 10% of the global population. Much effort has focused on identifying new therapeutic agents that inhibit pathological angiogenesis since 1971, when Judah Folkman published the hypothesis that tumor growth is angiogenesis-dependent and that its inhibition may be therapeutic. In 2004, the U.S. Food and Drug Administration approved the first antiangiogenic drug for the treatment of metastatic colon cancer, bevacizumab (Avastin, Genentech). This drug is a humanized monoclonal antibody that neutralizes the vascular endothelial growth factor. It is used in combination with chemotherapy, and its use began the era of antiangiogenesis therapy. Several new therapeutic agents have been added to the list of approved drugs, and clinical trials of new therapeutic options and antiangiogenic agents are ongoing [1].

But how anti-angiogenic therapies that damage the vasculature may shrink tumors and add months to patient survival but under some cir-

cumstances stimulate cancer invasion and metastasis. The perceived role of tumor vaccular biology is expanding from the structural lining of tumor-perfusing blood vessels to a stromal paracrine regulatory element and mechanisms of proliferation in cancer [2].

Vascular endothelial cells play as paracrine regulators of tumor progression has recently become appreciated. Healthy endothelial cells promote vascular repair and inhibit tumor invasiveness and metastasis; dysfunctional endothelial cells have the opposite effects activated endothelial cells will promote cancer cell inflammatory signaling and aggressive properties [2].

While physiologic angiogenesis is a tightly orchestrated process that is regulated by a balance of pro- and anti-angiogenic factors, tumor angiogenesis is erratic and irregular, with leaky vessels that are poorly formed. The tumor endothelial cells divide more rapidly than non-tumor endothelial cells and also express markers that the normal endothelial cells do not express [3].

Then tumor vascular architecture defects, or the tumor features itself leads to its proliferation and metastasis?

This study of embedding method was adopted to establish the rabbit VX_2 tumor model, the tumor characteristics of angiogenesis depending proliferation and metastasis, tumor vascular architecture were observed, and then given a review related about research progress of tumor vascular biology and tumor proliferation according to literature.

Materials and methods

Experimental animals: 36 New Zealand white rabbits, aged 3~4 months, weight 2~3 kg, male and female unlimited, Zhabei district central hospital animal center supplied, 36 rabbits were random divided into 2 groups: Experimental group: 18 rabbits liver were implanted with VX_2 tumor by surgery operation; Control group 18 rabbits performed the same surgery operation without tumor implantation, donor rabbits 2.

The study was approved by the ethics committee of Zhabei District Central Hospital.

Rabbit VX_2 squamous cancer cells was purchased from Funabashi company from Japan.

Experimental methods

Rabbit VX_2 tumor development and propagation

Development and propagation of the VX_2 cell line was performed according to previously according to the general cell culture technology. Flash-frozen rabbit VX_2 tumor samples were defrosted, the suspension trypan blue stained and counted death, living cells, guaranteed the cell vitality more than 95%, 10^6/ml living cells concentration was in the suspension, mixed in phosphate buffered saline media in a 1:1 ratio, took tumor suspension 0.5 ml, injected into abdominal subcutaneous tissue of donor New Zealand white rabbits for propagation. About 2-3 weeks after implantation, the donor rabbits were sacrificed and the abdominal subcutaneous tumors were excised and transected. Several 1-3 mm pieces of tumor were selected for surgical liver implantation and the remaining viable tumor was harvested from the specimen and strained in order to create a cell suspension using phosphate buffered saline media. The collected cells were centrifuged at 800 rotations per minute for five minutes, after which the supernatant was disposed of and the remaining cell pellet resuspended and mixed in phosphate buffered saline media in a 1:1 ratio. The new VX_2 cell samples were then immediately injected into the abdominal subcutaneous tissue of another rabbit in order to propagate the cell line.

VX_2 liver tumor implantation

All surgical VX_2 liver tumor implantations were performed under aseptic conditions with rabbits maintained under general anesthesia (with 3% pentobarbital sodium 30 mg/kg anesthesia through ear marginal vein). A laparotomy about 2 cm was created in the subxiphoid area, exposing the liver. Then, two 1-3 mm freshly harvested tumor fragments were implanted in the middle left hepatic lobe of each animal (n=18). One small stab incision was made by ophthalmic scissors about 0.5 cm deep in the liver abdomen side parenchyma, and the tumor pieces placed deep into incision. The incision was sutured continuously with 2-0 absorbable sutures one layer. The abdomen was closed in one layers using 1-0 absorbable sutures.

After the procedure, the animals were aroused and recovered, returned to cages, each experi-

ment rabbit was injected with 800,000 U penicillin and disinfection of incision within 3 d after operation for infection prevention, monitored daily for wound healing and appetite.

Tumor growth monitoring

2 experiment rabbits were sacrificed to observe tumor growth after inoculation 7, 14, 21, 28, 35, 42 d. Tumor diameters were measured with vernier caliper, took tissue samples from local lymph nodes, lung, kidney, etc that may be possible metastasis. Experiment rabbits survival status was recorded.

The maximum diameter (A) and transverse diameter (B) of tumor were separately recorded. The tumor size (V) was calculated as "$V=A\times B^2/2$". The size of tumors in livers was measured macroscopically.

Planting after 1 week, liver ultrasound examination was performed every other day, monitoring of tumor growth size, shape, number of lesions, the echo intensity.

Tumor cancer pathological observation

The tumor tissues were fixed in 10% neutral formaldehyde, conventionally paraffin embedded, sectioned, and placed on slides. Then, one slide was stained with hematoxylin and eosin (HE), one slide was stained with Victoria blue to observe elastic fibers and Ponceau's histochemical stain, and one slide was biotin-labelled and stained with ulex europaeus agglutinin (UEA) I. All slides were observed under an optical microscope.

Elastic fiber staining

The reagent preparation methods for Victoria blue and Ponceau's histochemical staining were described previously [4].

Elastic fiber staining method: The biopsy was dewaxed in water. A section was washed in 70% ethanol for 2 min, and then incubated with the Victoria blue solution for 0.5~2 h. The Spring red S dropped slice 2 min, flushed extra dyeing liquid 2 times with anhydrous ethanol directly. The slice was dried in the air, Xylene transparent, neutral gum cementing.

For the slide that was dyed for elastic fiber damage, a microscopic micrometer was used to measure the tumor vascular caliber.

The microscopic micrometer had two parts that were used cooperatively: eyepiece micrometer and stage graticules. For the microscopic measurements, first, the stage graticules were used to measure the length of each grid in the ocular field; then, the eyepiece micrometer was used to measure blood vessel diameter. At 100× and 400× magnifications, each eyepiece micrometer represented 4.8 μm and 1.2 μm, respectively. We first looked for blood vessels at 40× magnification and then looked for vascular damage at 400× magnification. For each specimen, 5 horizons were counted, and the average vascular caliber of HIFU damage was calculated.

Tumor-derived vascular endothelial UEA I staining

The avidin-biotin peroxidase complex (ABC) method was adopted. Biotin-labelled UEA I (Beijing Zhongshan Biotechnology Co., LTD) was used at a working concentration of 20 μg/ml. UEA can be combined with diaminobenzidine (DAB) coloration of endothelial cells.

UEA staining and microvessel density count: Isolated endothelial cells and cell clusters that were positively stained with UEA with or without visible lumina were counted as separate microvessels. Blood vessels that had a thick muscle layer or a vascular diameter greater than eight red blood cells were examined by HE staining. Elastic fibers were stained and observed separately. The tumor microvessel region was examined at 100× magnification under a light microscope. Microvessel density was examined at 400× magnification under a light microscope. The five highest microvessel density counts per tumor region (called "hot spots") were averaged and used for the statistical analysis. The student's T-test was applied for comparisons between the two groups.

Ultrastructural observation

Specimens were cut into 1 mm^3 pieces. Then, half of the piece was prepared by the CQR-1 type ultra-microtome method, and ultrathin sections were prepared after positioning. The sections were stained with uranyl acetate and lead nitrate and observed and photographed by H-600 transmission electron microscopy.

The data in the present study were showed as mean ± SD. T-student test and correlation anal-

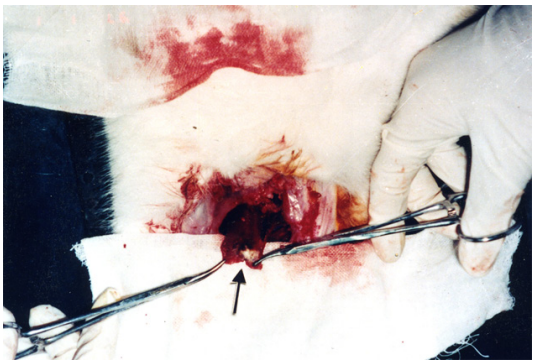

Figure 1. The rabbit liver tumor was visible 1 week after implant.

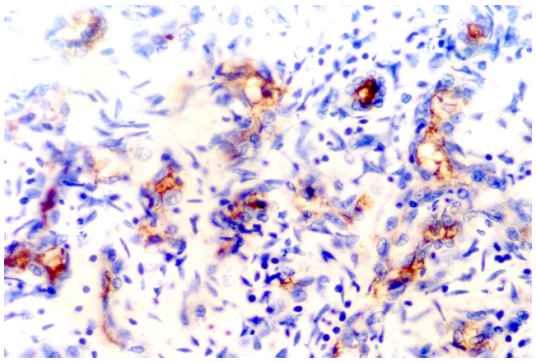

Figure 2. Hepatic VX_2 tumor in rabbit, the endothelial cells UEA I staining positive (400 times HPF).

ysis were used to analyze the variance in different groups, SPSS 19.0 software (SPSS, Inc.) was used for the statistical analyses of the data. The accepted level of significance was set at $P<0.05$.

Results

Ultrasonic monitoring of tumor growth

After the transplant 7~10 d found no tumor in ultrasound images. After 10~14 d tumor implanted, 16 experiment rabbits were found each have a specific tumor nodules, size in the range of 0.5~1.0 cm in ultrasonography forming quasi-circular echo, the boundary was not clear, including two of the nodules were hyperechogenicity nodules, the remaining 14 present hypoechoic nodules, two animals liver had mild heterogeneity echo, not sure whether there were tumor or nodules. Control group found no tumor grew by ultrasonic monitoring.

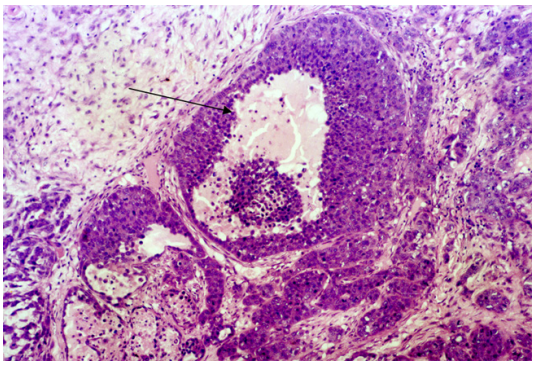

Figure 3. Hepatic VX_2 tumor in rabbit tumor, ischemic necrosis in center of tumor nodes. Hematoxylin-eosin staining, (400 times HPF).

Animals dissection and tumor growing characteristics

2 experiment rabbits were sacrificed and dissected after inoculation 7, 14, 21, 28, 35, 42 d after tumor implanted, tumor implant success rate was 100%, no natural fade phenomenon was found. 18 experimental rabbits VX_2 tumor nodules were found in the middle left hepatic lobe, a total of number was 51, 10 tumor nodules were in diameter 0.5~1.0 cm, 25 tumor nodules in 1.3~2.5 cm, 16 tumor nodules were over 2.5 cm. Tumor nodules were ovoid in shape, or a fusion of irregular nodules; the nodules was solid without capsule form. Tumor nodules section was pale, fish meat like and texture coarse; the embedding site and surrounding tissues was without adhesion, infiltrating nests inside liver without a clear boundary with liver parenchyma.

Control group found no tumor grew after 2 experiment rabbits were sacrificed and dissected (see experiment rabbits survival status part).

Microscopic pathological examination, all of tumor nodules were poorly differentiated squamous carcinoma, formed a small amount of nests.

Tumor nodules diameter in 0.3~0.5 cm after implanted 1 week (**Figure 1**, n=2), diameter in 2~3 cm in 3~4 weeks. When tumor nodules diameter was more than 1cm, its center may have visible ischemic necrosis.

Table 1. List of tumor blood vessel growth situation ($\bar{x} \pm s$)

Implanted days	0	7	13	21	28	35	42	Pearson Correlation
Tumor blood vessel growth	No	Yes	Yes	Yes	Yes	Yes	Yes	
Source of tumor blood supply	Hepatic sinusoid	HSTBV	HSTBV	HSTBV	HSTBV	HSTBV	HSTBV	
Vascular caliber μm	0	95±23	115±34	150±32	170±25	190±26	200±13	P=0.848
Volume of original tumors (cm^3)	0.15±0.11	0.82±0.10	1.2±0.12	3.5±0.21	5.6±0.25	7.3±1.26	9.3±1.11	S=0.033

HSTBV: hepatic sinusoid and tumor blood vessels; P: Pearson Correlation; S: Sig. (2-tailed).

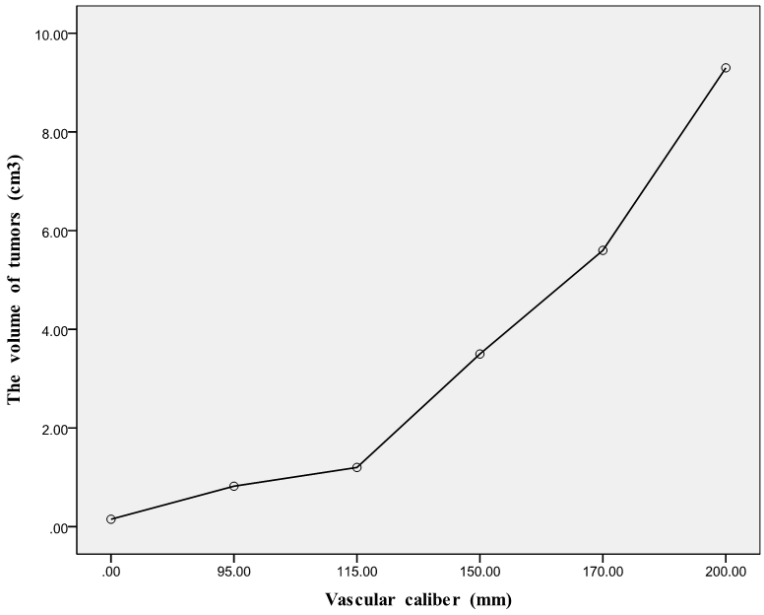

Graph 1. The volume of original tumors change with vascular caliber.

Tumor blood vessel growth

Endothelial cells UEA I detection

The microvessel UEA I staining was positive, uneven distribution in the tumor tissue, high density of blood vessels called "hot spots", formed a lumen, or only a single endothelial cell or cluster of endothelial cells (**Figure 2**, n=18). The average vascular density count of 18 experimental rabbits under 400 times light microscope were 43.17 ± 8.68/vessels/High Power Field (HPF). There was no tumor growth in Control group, tumor vascular density count was 0, there is significant difference between two groups (t=21.102, P<0.000).

Microscope pathological observation, 3 d after tumor implanted, there were not found the tumor blood vessels growth, nutrition supply mainly from liver blood sinus. 5 d after tumor implant found visible tumor tissue nutrition supply mainly from the new tumor blood vessels and the liver blood sinus, the vascular diameter average in 130 μm. Tumor grew faster after establishing blood supply. Ischemic necrosis was found in the center of tumor mass without enough blood supply while tumor grew rapidly after tumor implanted 14 d (**Figure 3**, n=3), **Table 1**.

When implanted tumors volume up to 0.82 cm^3, angiogenesis began to provide nutrition for tumor. The tumor grew acceleration with tumor angiogenesis, volume of original tumors (cm^3) was correlated with vascular caliber (mm) (Pearson correlation= 0.848: Sig.=0.033), see **Table 1**, **Graph 1**.

Tumor hematogenous metastasis

The experiment rabbits were dissected found that the tumor infiltrated into liver blood sinus after tumor implant 7 d first (**Figure 4A**, n=3); then tumor invaded the blood vessels within the connective tissue after tumor implant 21 d (**Figure 4B**, n=2); the tumor spread to the liver capsular vein after tumor implant 28 d (**Figure 4C**, n=2).The tumor was found lung metastasis (**Figure 5A**, **5B**, n=2) and kidney metastasis (**Figure 6A**, **6B**, n=2) after implanted 3~4 weeks. The tumor was discovered widely abdominal cavity invasion associated with experimental animal systemic failure and death after tumor implant 42-49 d (**Figure 7**, n=6). Tumor hematogenous metastasis course see **Graph 2**.

2 experiment rabbits were sacrificed and dissected after inoculation 7, 14, 21, 28, 35, 42 d after tumor implanted (n=12), the survival time was recorded in the rest of 6 experiment rabbits, 4 experiment rabbits died in 7 week, 2 experiment rabbits died in 8 week. It was found

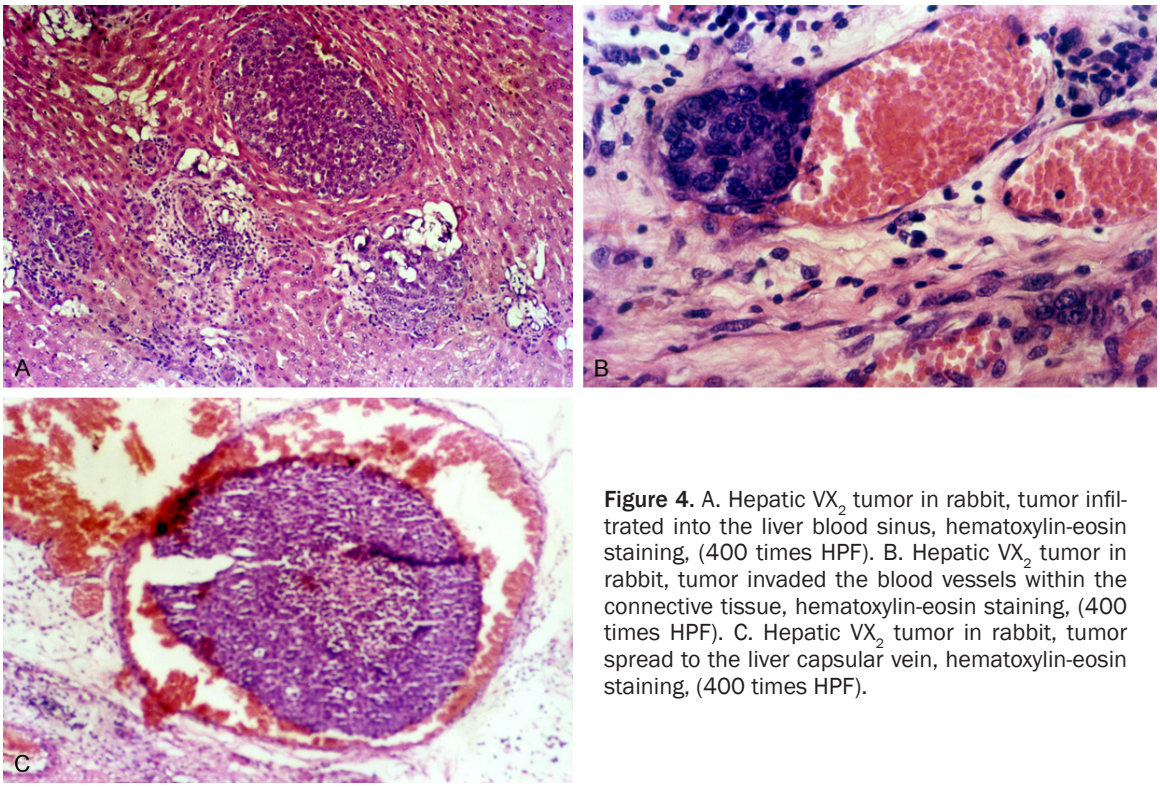

Figure 4. A. Hepatic VX_2 tumor in rabbit, tumor infiltrated into the liver blood sinus, hematoxylin-eosin staining, (400 times HPF). B. Hepatic VX_2 tumor in rabbit, tumor invaded the blood vessels within the connective tissue, hematoxylin-eosin staining, (400 times HPF). C. Hepatic VX_2 tumor in rabbit, tumor spread to the liver capsular vein, hematoxylin-eosin staining, (400 times HPF).

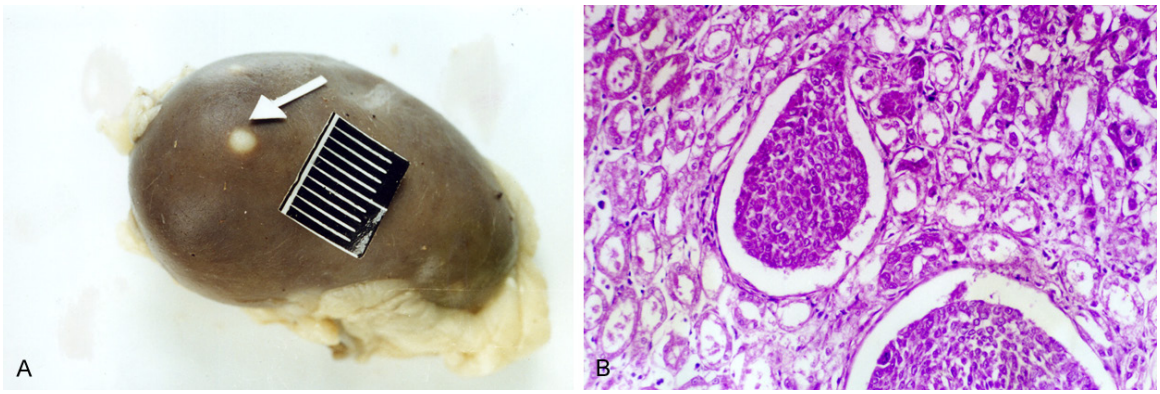

Figure 5. A. The kidney metastasis of VX_2 rabbit implant liver tumor. B. The kidney metastasis of VX_2 carcinoma, hematoxylin-eosin staining, (400 times HPF).

no tumor growing when 2 rabbits were sacrificed and dissected in Control group after operation 7~8 week. Experiment rabbits survival status see **Graph 3**.

Elastic fiber staining

Blood vessels elastic fiber histochemical staining presented blue, collagen fibers presented red with pale yellow background. Tumor blood vessels internal and external elastic plate was intact without vessels elastic fiber architecture defect found (**Figure 8A**). Tumor vascular diameter all within 200 μm, **Table 1**.

Vascular endothelial cells organelles of tumor were integrity without endothelial cells architecture defect found by transmission electron microscopy (**Figure 8B**).

Discussion

The choice of animal tumor model

Ideal tumor animal models require as much resemble as possible in location, histologic

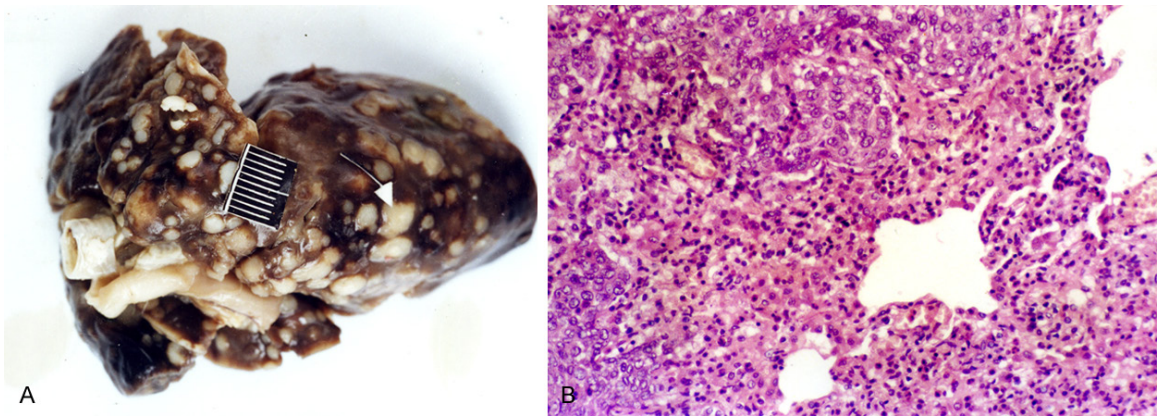

Figure 6. A. The lung metastasis of VX_2 rabbit implant liver tumor. B. The lung metastasis of VX_2 carcinoma, hematoxylin-eosin staining, (400 times HPF).

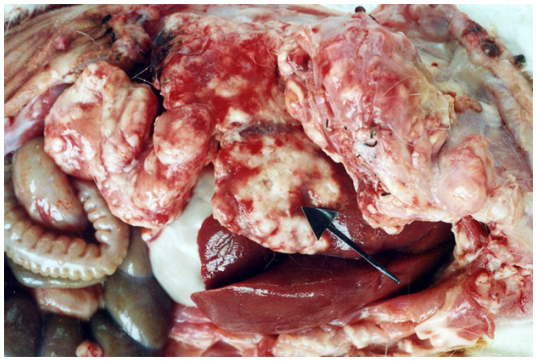

Figure 7. The abdominal cavity metastasis of VX_2 rabbit implant liver tumor.

type, etiology, pathogenesis with human tumor biological behavior [5].

VX_2 tumor cell lines came from Shope virus (rabbit papilloma virus) induced squamous cell carcinomas. The tumor has lost the dependence of the virus and kept the characteristics easy to hand down from generation to generation as an experimental tumor and become a portable tumor strains. It can grow in different organs of the rabbits with characteristics of high rate infiltrating growth and metastasis, so embedding method in this experiment is adopted to establish the rabbit VX_2 liver tumor model [5].

Our rabbit liver grafting tumor model can monitor the whole course of hepatic tumor growth and lung, kidney metastasis, widely abdominal cavity invasion associated with animal systemic failure and death.

Tumor angiogenesis dependent growth

Angiogenesis is process formation of new blood vessels from existing vascular endothelium. Tumors as small as a few cubic millimeters in size are not able to continue to grow without vigorously inducing new blood vessel formation. Tumor grows acceleration, almost exponential growth after angiogenesis [6].

From the above rabbits tumor model found, when implanted tumors volume up to 0.82 cm^3, angiogenesis began to provide nutrition for tumor. The tumor grew acceleration with tumor angiogenesis, volume of original tumors was correlated with vascular growth.

Our rabbit liver grafting tumor model found after tumor implanted nutrition supply mainly came from liver blood sinus first; then tumor nutrition supply came from the new formed tumor blood vessels and the liver blood sinus. Due to the growth of blood vessels can't keep up with the tumor cell growth, so the tumor nodules center may have ischemic necrosis.

Five main different principal cellular mechanisms under the heading of tumor angiogenesis. These include [7]:

Sprouting angiogenesis, the sprouting of capillaries come from preexisting vessels.

Vascular co-option describes the infiltration of tumor cells invade into normal tissue and the adoption of the pre-existing vasculature. Vascular co-option may be viewed as part of the invasive phenotype that is intrinsic to

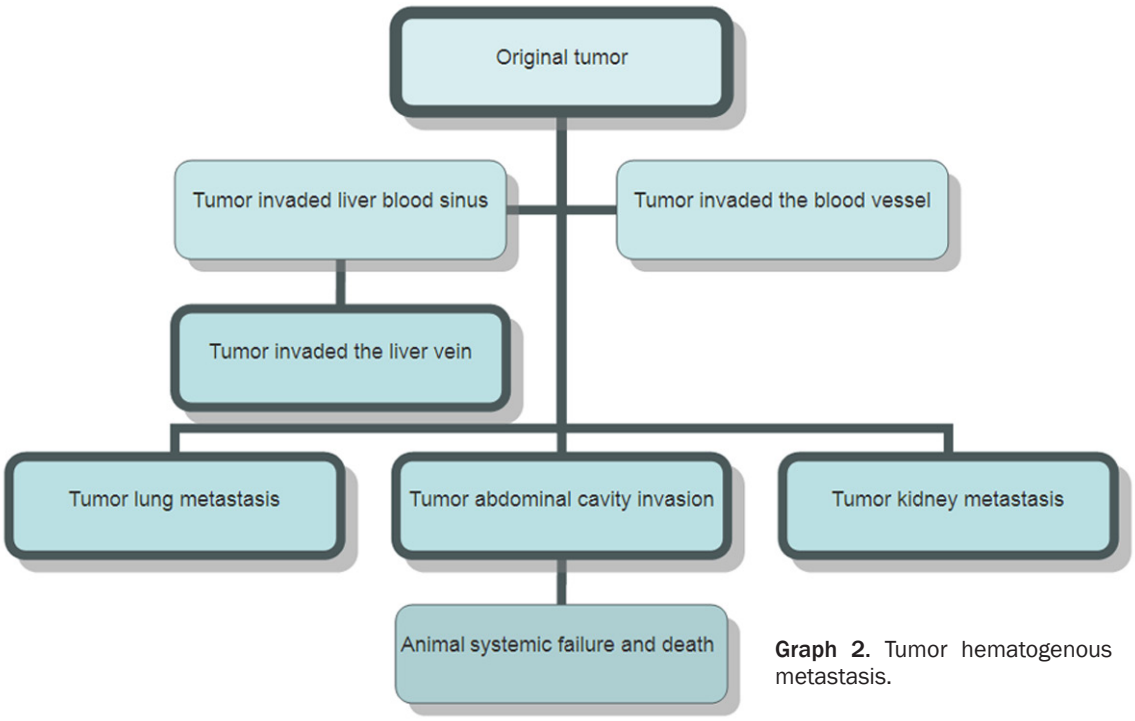

Graph 2. Tumor hematogenous metastasis.

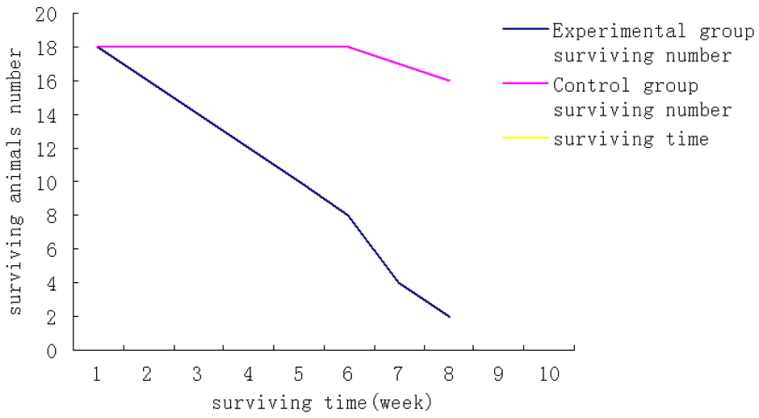

Graph 3. Experimental rabbits surviving status.

tumor-rather than an active vascular process. Invoking the process of vascular co-option aligns well with the known migratory pattern of tumor cells along vessels.

Vessel intussusception describes the formation of a new vessel by vascular invagination, intra-luminar pillar formation and splitting. Vascular intussusception has initially been described in physiological vascular development but more recently has been expanded to experimental tumors. It has been suggested that sprouting angiogenesis may switch to vascular intussusception to allow rapid development of new vessels. The molecular mechanisms that drive vascular intussusception are currently poorly understood.

Vasculogenic mimicry is defined as a process where tumor cells replace endothelial cells and form a vessel with a lumen. This phenomenon was first described (mainly based on PAS staining) in a subset of aggressive uveal melanomas and later in other types of cancer but its overall occurrence and significance, if any, is highly controversial. Moreover, it is unclear whether vasculogenic mimicry represents an active process (e.g., cancer cells actively forming the vascular lumen) or whether vasculogenic mimicry is a consequence of vessel regression.

Bone marrow derived vasculogenesis describes the recruitment of circulating endothelial precursor cells to the tumor, their integration into

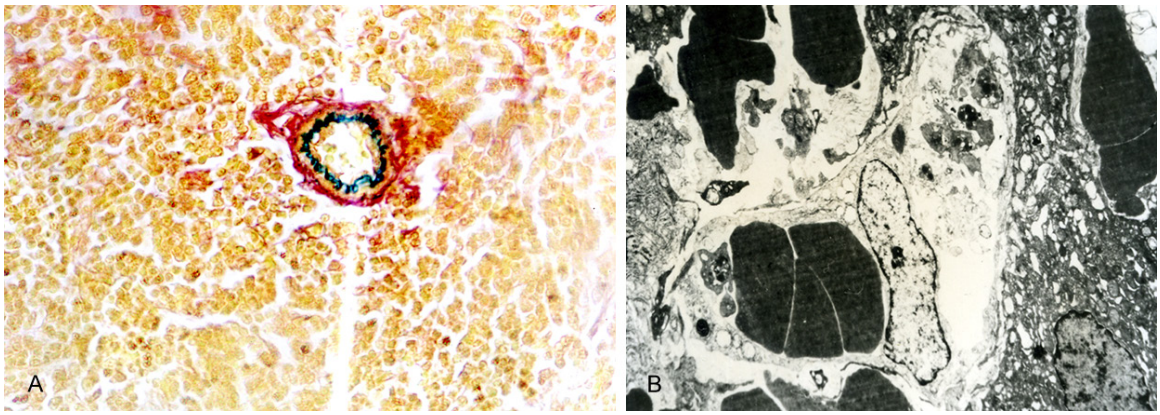

Figure 8. A. Tumor blood vessel in internal and external elastic plate integrity. (Blood vessels elastic fiber and collagen fiber histochemical double staining, elastic fibers appears blue, collagen fiber red, background pale yellow, tube diameter in 50 μm, 400 times HPF). B. Vascular endothelial cells organelles of tumor were integrity, transmission electron microscopy, 4000 times.

the vessel wall and their terminal differentiation into an endothelial cell.

We found tumor infiltrated into liver blood sinus, invaded into the blood vessels within mesenchyme, spread to the liver capsular vein, but did not found tumor vascular formation as the same described as Vascular co-option, Bone marrow derived vasculogenesis and so on.

So from the above listed mechanisms of tumor angiogenesis, we assume sprouting angiogenesis maybe the main operational in VX_2 rabbits tumor because pathology examination found after tumor implanted nutrition supply mainly came from liver blood sinus first; then tumor nutrition supply came from the new formed tumor blood vessels.

VX_2 tumor nodules center necrosis may have lumen formation, it is maybe a process of Vasculogenic mimicry? But it needs further exploration.

The role of tumor endothelial cells

UEA I staining vascular (endothelial cells) density count is the commonly method used to observe tumor angiogenesis status. The average vascular density count of the above 18 experimental rabbits were calculated. It is suggests the tumor angiogenesis very actively.

Endothelial cells (EC) line every vessel, sensing and biochemically responding to flow from above, strain and stress from below and local density at their periphery. These vantage points allow regulation of multiple aspects of local biology. The dynamic response of the EC secretome to microenvironmental perturbations allows the EC to provide a range of paracrine effects. This capability, entrenched in understanding of vascular disease, has re-emerged in tumor biology [2, 7].

Endothelial cells play as paracrine regulators of tumor progression has recently become appreciated. Healthy endothelial cells promote vascular repair and inhibit tumor invasiveness and metastasis; dysfunctional endothelial cells have the opposite effects. Dysfunctionally activated endothelial cells promote cancer cell inflammatory signaling and aggressive properties. Factors released from quiescent ECs induce balanced inflammatory signaling, correlating with decreased proliferation and invasiveness, factors released from dysfunctional ECs robustly activated NF-κB and STAT3 signaling within cancer cells, correlating with increased in vitro invasiveness and decreased proliferation and survival. Furthermore, matrix-embedded dysfunctional endothelial cells stimulated intratumoral pro-inflammatory signaling and spontaneous metastasis [2, 7].

Epithelial to mesenchymal transition (EMT) contribute to tumor proliferation: When EMT occurs in adult tissues in response to injury or during tumorigenesis, epithelial cells change morphological appearance, from an ordered structure with apical and basal polarity to a less ordered, migratory fibroblastic shape. The

Snail family of transcription factors (Snail1/Snail and Snail2/Slug) is closely associated with EMT, because they suppress epithelial cadherin (E-cadherin) expression, which normally facilitates cell-cell interactions, providing polarity cues and preventing dissemination. Snail associated EMT is normally under stringent regulation, but when that is lost, cancer may appear. Increased expression of Snail and Slug protects cells from death induced by the loss of survival factors or by apoptotic stimuli. Elevated Snail1/2 results in increased protection from DNA damage, increased resistance to chemotherapeutic agents and radiation therapy. Snail and Slug may also affect a cell's response to genotoxic stress, increasing DNA damage, which then may contribute to cancer development [2, 8].

The impact of stromal cells on tumor growth

Tumor tissue containing tumor cells and stromal components (including its suply vascularities) in tumor microenvironment contributes to tumor progression and metastasis. Broadly speaking, the relationship of tumor vascularities and tumor cells is as the same as the relationship of tumor cells and their stromal components.

Stromal components in tumor microenvironment contribute centrally to tumor progression and metastasis. Reciprocal interactions occur between neoplastic cells and stromal components leading to coevolution. In this context, either stromal cells support transformation of epithelial cells, or transformed tumor cells engage stromal cells, and the altered environment can influence the metastatic, dormancy related, and stem-like potential of tumor cells. So do the above rabbits VX_2 tumor [8].

The stromal compartment of the tumor is complex, consisting of inflammatory/immune cells, endothelial cells (vascular), pericytes, fibroblasts, adipocytes and extracellular matrixcomponents (e.g., collagen, fibronectin, laminin and proteoglycan complex). Tumor infiltrating inflammatory cells release EGF, VEGF, fibroblast growth factor-2 (FGF-2), chemokines, cytokines, and proinvasive matrix degrading enzymes to promote tumorigenesis. Continued tumor growth and progression is mediated by the "angiogenic switch", which occurs in response to VEGF and FGF-2 secreted from tumor cells, resulting in angiogenesis. Fibroblasts in the tumor microenvironment provide the structural framework of the stroma. Fibroblastsremain quiescent, but they proliferate during wound healing, inflammation and cancer. Paracrine factors from tumor cells activate fibroblasts to become "cancer associated fibroblasts" (CAF). CAFs secrete factors that modulate tumor growth and modify the stroma to facilitate metastasis and attenuate responses to anticancer therapies. Thus, tumor stromal crosstalk is important when developing therapeutic options, since tumor centric approaches may not work in a stroma rich tumor microenvironment [1, 2, 7, 8].

The cancer cell embodies characteristics that permit survival beyond its normal life span and to proliferate abnormally, so do the above rabbits VX_2 tumor. VX_2 tumor nodules center necrosis is a common phenomenon during tumor proliferate, one explanation is due to the growth of blood vessels can't keep up with the tumor cell growth, so the tumor center may have ischemic necrosis. Then are there any other explanation?

Hypoxia and tumor proliferation

Cancer development results from the selection of cells with mutation(s) that provide survival and proliferative advantages. Normal barriers to proliferation are overcome as clones adapt to an ever changing hostile microenvironment, where low oxygen tension, low glucose levels, and an acidic extracellular pH (all of which increase genetic instability) are found. The hypoxia inducible factors (HIF-1 and HIF-2) are up regulated in response to these conditions [1, 2, 6, 8].

Premalignant nodules (such as the above VX_2 tumor implanted at once) are mostly devoid of blood vessels which limits the diffusion of substrates across the basement membrane from the local blood supply. Adaptation to these conditions is critical in the transition from a benign nodule to malignancy. As such, carcinoma in situ (CIS) becomes malignant following rupture of the basement membrane and invasion into the surrounding tissue, which may be facilitated by increased acid production. Hypoxia may promote CIS progression by selecting for cells that are resistant to extra cellular acidosis and those with upregulated glycolysis. Thus, the

transition from preinvasive to invasive tumor may be closely linked to the CIS microenvironment [1, 2, 6, 8].

In inflammation related carcinogenesis, altered tissue architecture due to necrosis and the development of hypoxia attracts inflammatory responses. Thus, in the above VX_2 tumor nodules center HIFs link hypoxia, chronic inflammation, and tumor progression by reprogramming tumor cells, macrophages and other cells during cancer development [1-3, 6, 8].

The tumor center necrosis and tumor autophagy

In normal cells, basal autophagy is a mechanism that maintains cellular homeostasis by removing protein aggregates and damaged organelles, whereas starvation induced autophagy prolongs cell survival by recycling amino acids and energy, which are both important for cellular fitness and preserving viability. The basal level of autophagy increases in cancer cells to withstand stresses due to dysregulated signaling mediated proliferation, enhanced glycolysis, hypoxia, and to maintain cancer cells in a state of quiescence. However, autophagy can promote tumor cell survival or cell death depending upon the tumor type, and thus, the implications of induced autophagy are not completely understood. It can be modulated therapeutically, either promoting survival or death [7, 8].

So, the above VX_2 tumor nodules center necrosis maybe a tumor autophagy phenomenon.

Survival and growth of cancer stem cells (CSCs)

Cells stem cells (SCs) and CSCs share similar characteristics of "stemness", quiescence, self renewal, the ability to produce differentiated progeny, resistance to apoptosis, and chemoresistance. What distinguishes CSCs from adult SCs is the aberrant regulation of these processes in the former, resulting in altered cell fate and unregulated cell growth [1, 6, 8].

The tumor mass contains a small proportion of CSCs that initiate/maintain malignant growth and differentiated progeny of these CSCs that do not. Adult SCs divide asymmetrically, giving rise to a differentiated daughter cell and progenitor cell capable of a limited number of additional cell divisions. In contrast, CSCs divide symmetrically into progenitor cells that possess an unlimited replicative potential that allows them to undergo an indefinite number of cell divisions. The latter may explain tumor relapse after initial therapy, where most of mature tumor cells are eliminated, while therapy resistant CSCs become reactivated and proliferate. Initial tumor responses might mean little if CSCs determine outcome [2, 6, 8].

Targeting cell cycle proteins in sustained proliferative signaling: The G1phase of the cell cycle is the only time that a cell can respond to extra cellular cues, and progression depends on the balance of proliferative and antiproliferative signals. In the presence of "go" signals, progression into S phase occurs; in the presence of "stop" signals, the cell arrests in G1. Thus, cancer can be thought of as a disease of the cell cycle: where a cancer cell ignores the "stop" signals and does not wait for the "go" signals. The result is excessive DNA replication, which increases the likelihood of replication induced mutations and telomere degeneration, further disabling other hallmark pathways [2, 3, 8].

So from the above literatrue and the above VX_2 model we can found, VX_2 tumor CSCs as an internal factor determines VX_2 tumor proliferation, metastasis or autophagy (necrosis). It is acts as external factors such as tumor hypoxia microenvironment, angiogenesis, endothelial paracrine, epithelial to mesenchymal transition and so on. Reciprocal interactions occur between neoplastic cells and stromal components leading to coevolution. Angiogenesis and tumor proliferation are interdependent, forming a chaotic cycle.

Tumor hematogenous metastasis

Vascular stroma not only provides nutrients and oxygen to remove metabolites, but also the formation of new vessels become pathways of regeneration and tumor blood vessels metastasis.

It is assumed the general steps of the tumor metastasis as following: (1) Primary tumor proliferates and generates new blood vessels in the tumor; (2) Tumor cells invade adjacent to the basement membrane, matrix and normal cells; (3) Tumor cells enter blood vessels or the

lymphatic vessels and survive in the circulation system; (4) Tumor cells form embolism, stay in the target tube capillary in distant and proliferate; (5) Tumor cells cross through the blood vessels or the lymphatic vessels and form micro metastases in the target organ; (6) New angiogenesis in tumor stroma, metastatic tumor grows rapidly [9].

It can be seen from our above rabbits model, the rabbits VX_2 liver tumor first infiltrated into liver blood sinus, invaded the blood vessels within the connective tissue, and then spread to the liver capsular vein. The tumor was found lung and kidney metastasis after implanted 3~4 weeks. At last widely abdominal cavity invasion associated with experimental rabbits systemic failure and death after tumor implant 42~49 d.

Then tumor vascular architecture defects, or the tumor features itself leads to its proliferation and metastasis?

It can be seen from above rabbits VX_2 tumor model, the elastic fiber dyeing found tumor blood vessels internal and external elastic plate intact. Vascular endothelial cells organelles of tumor were integrity without endothelial cells architecture defect found. So no tumor vascularity architecture defect was found in our pathological observation. Other methods may be more effective to discover tumor vascularity architecture defect, it reported, improved high-resolution imaging techniques are increasingly being implemented and tested in clinical trials to provide serial measures of tumor blood perfusion, vascular volume, and vascular permeability as methods to better understand the modes of action of antiangiogenic cancer therapy. It needs further exploration [10, 11].

Future prospects for anti-angiogenic therapy

Tumors as small as a few cubic millimeters in size are not able to continue to grow without vigorously inducing new blood vessel formation. As a result, tumor starvation through interference with tumor blood supply has become a well-recognized approach of cancer therapy. Conceptionally, antiangiogenic therapy pursues a strategy that is directed against the vascular constituent of the tumor stroma rather than the conventional target, which is the tumor cell itself. The tumor microenvironment as a primary target of such a stromal therapy approach carries the prospect of being less prone to resistance mechanisms due to genetic stability [1, 12].

The angiogenic cascade is subject to very dynamic and complex regulation. A large number of proangiogenic and antiangiogenic factors have been demonstrated to control angiogenesis.

It is now evident that the entire process of tumor-induced angiogenesis appears to be far more complex than initially envisioned. Moreover, the idea that blockade of tumor angiogenesis is able to inhibit tumor growth in vivo has been confirmed in principal in both experimental and clinical settings; however, current evidence suggests that cancer cells are able to circumvent anti-angiogenic therapy and develop resistance to targeted mono-therapy [1, 7, 12].

Documented undesired effects of bevacizumab therapy include hypertension, induction of bleeding disorders and deep venous thrombosis. In addition to the above-mentioned adverse effects of anti-VEGF treatment, pre-clinical and clinical reports suggest that cancer cells may develop resistance to antiangiogenic therapy by different mechanisms that include (1) switch to a pro-migratory phenotype, (2) up-regulation of other pro-angiogenic molecules and (3) the increased recruitment of myeloid cells that support tumor growth [1-3, 12].

Since antiangiogenic monotherapies may only act as cytostatic agents, making objective response measurements like tumor shrinkage, or simply inhibit further growth and spread. Then further studies are needed to examine the effect of vessel “normalization”, whereby the tumor vessels become more organized and blood flow is improved and if improved tumor delivery of chemotherapeutics could be achieved [1-3, 9, 12].

“Vascular normalization” states that anti-angiogenic (e.g., Bevacizumab) treatment merely affects the immature vasculature and leaves the mature vessels unaltered. As such, a “normalized” vasculature results as a consequence of anti-VEGF treatment, leading to increased perfusion of the tumor and subsequent

increase of oxygenation. Vascular normalization is thought to interrupt the vicious circle that is driven by hypoxia and that leads to upregulation of VEGF, resulting in the growth of immature-partly unperfused-vessels and a subsequent increase in tumor hypoxia [1, 3, 9, 12].

Current directions of targeted antiangiogenic cancer therapy

In particular, two trends of targeted antiangiogenic cancer therapy have become apparent. Firstly, antiangiogenic compounds with therapeutic activity in advanced disease are increasingly being tested in the adjuvant clinical setting, vessel "normalization" followed by cytotoxic chemotherapy and/or radiotherapy should be the ultimate goal of any antiangiogenic therapy.

Secondly, there is a clear tendency at present to combine different antiangiogenic agents to accomplish a more comprehensive approach in blocking tumor angiogenesis.

Facing limitation of antiangiogenic monotherapies (e.g., Bevacizumab), other treatment methods such as high intensity focused ultrasound (HIFU) maybe recommend. HIFU caused coagulative necrosis in the tumor tissues and their vascularities. We will report these treatment results on other articles.

To sum up from the above literature review and our VX_2 tumor model, angiogenesis and tumor proliferation are interdependent, forming a chaotic cycle. The mechanism of tumor proliferation and metastasis are associated with changes in cell phenotype that include epithelial to mesenchymal transition (EMT) and cell migration, resulting in local regions of hypoxia that promote the survival and growth of tissue stem cells, as well as angiogenesis. Autophagy also promotes the survival of preneoplastic and tumor cells under stressful conditions. Curent antiangiogenic monotherapies is act as cytostatic agents in clinic.

This study only observed some phenomena of the liver implanted tumor proliferation and metastasis vascular dependence, characteristic of tumor vascular architecture, its detailed mechanism need further exploration and discovery.

It can be seen from the above experiment, proliferation and metastasis of rabbit VX_2 hepatic carcinoma was correlated with tumor vascular growth, no tumor vascular architecture defect was found in our pathology observation, it need further exploration. Angiogenesis and tumor regeneration are interdependent, forming a chaotic proliferation cycle. While it is very important to understand mechanism of tumor proliferation, angiogenesis and course of tumor cells invading into blood vessels for we make strategy of anti-tumor angiogenic treatment.

Acknowledgements

Conception, design, acquisition of data, drafted the manuscript by Liming Guan. We thank Professor Zhibiao Wang, Professor Feng Wu (Chongqing Medical University) for their revising the article critically for important intellectual content. We also thank the doctors and nurses of Zhabei District Central Hospital for providing useful advice and cooperation. The author(s) received no financial support for the research, authorship, and/or publication of this article.

Disclosure of conflict of interest

None.

Address correspondence to: Liming Guan, Department of Obstetrics and Gynaecology, Zhabei District Central Hospital, No. 619, Zhonghuaxin Road, Zhabei District, Shanghai 200000, China. E-mail: limingguan5@163.com

References

[1] Staton CA, Brown NJ, Reed MW. Current status and future prospects for anti-angiogenic therapies in cancer. Expert Opin Drug Discov 2009; 4: 961-79.

[2] Franses JW, Drosu NC, Gibson WJ, Chitalia VC, Edelman ER. Dysfunctional endothelial cells directly stimulate cancer inflammation and metastasis. Int J Cancer 2013; 133: 1334-44.

[3] Cook KM, Figg WD. Angiogenesis inhibitors: current strategies and future prospects. CA Cancer J Clin 2010; 60: 222-43.

[4] Gong ZJ, Zhan R. Pathological tissue production and dyeing technology, Version 1. Shanghai: Shanghai Science and Technology Publishing House; 1994. pp. 66-88.

[5] Rous P, Kidd JB, Swith WE. Experiments on the cause of the rabbit carcinoma derived from virus-induced papilloma: II. Loss by the VX_2 carcinoma of the power to immumize hosts against

the papilloma virus. J Expl Med 1995; 96: 159-174.
[6] Gille J. Antiangiogenic cancer therapies get their act together: current developments and future prospects of growth factor- and growth factor receptor-targeted approaches. Exp Dermatol 2006; 15: 175-86.
[7] Plate KH, Scholz A, Dumont DJ. Dumont. Tumor angiogenesis and anti-angiogenic therapy in malignant gliomas revisited. Acta Neuropathol 2012; 124: 763-775.
[8] Feitelson MA, Arzumanyan A, Kulathinal RJ, Blain SW, Holcombe RF, Mahajna J, Marino M, Martinez-Chantar ML, Nawroth R, Sanchez-Garcia I, Sharma D, Saxena NK, Singh N, Vlachostergios PJ, Guo S, Honoki K, Fujii H, Georgakilas AG, Bilsland A, Amedei A, Niccolai E, Amin A, Ashraf SS, Boosani CS, Guha G, Ciriolo MR, Aquilano K, Chen S, Mohammed SI, Azmi AS, Bhakta D, Halicka D, Keith WN, Nowsheen S. Sustained proliferation in cancer: Mechanisms and novel therapeutic targets. Semin Cancer Biol 2015; [Epub ahead of print].
[9] Naveen S. Vasudev, Andrew R. Reynolds, Anti-angiogenic therapy for cancer: current progress, unresolved questions and future directions. Angiogenesis 2014; 17: 471-494.
[10] McDonald DM, Choyke PL. Imaging of angiogenesis: from microscope to clinic. Nat Med 2003; 9: 713-725.
[11] Schirner M, Menrad A, Stephens A, Frenzel T, Hauff P, Licha K. Molecular imaging of tumor angiogenesis. Ann N Y Acad Sci 2004; 1014: 67-75.
[12] Yadav L, Puri N, Rastogi V, Satpute P, Sharma V. Tumour Angiogenesis and Angiogenic Inhibitors: A Review. J Clin Diagn Res 2015; 9: XE01-XE05.
[13] Giordano G, Febbraro A, Venditti M, Campidoglio S, Olivieri N, Raieta K, Parcesepe P, Imbriani GC, Remo A, Pancione M. Targeting angiogenesis and tumor microenvironment in metastatic colorectal cancer: role of aflibercept. Gastroenterol Res Pract 2014; 2014: 526178.